Journal of Hazardous Materials 159 (2008) 574–579

Contents lists available at ScienceDirect

Journal of Hazardous Materials

journal homepage: www.elsevier.com/locate/jhazmat

Malachite green adsorption by rattan sawdust: Isotherm, kinetic and mechanism modeling

B.H. Hameed [a,*], M.I. El-Khaiary [b]

[a] School of Chemical Engineering, Engineering Campus, Universiti Sains Malaysia, 14300 Nibong Tebal, Penang, Malaysia
[b] Chemical Engineering Department, Faculty of Engineering, Alexandria University, El-Hadara, Alexandria 21544, Egypt

ARTICLE INFO

Article history:
Received 31 December 2007
Received in revised form 17 February 2008
Accepted 19 February 2008
Available online 23 February 2008

Keywords:
Adsorption
Batch processing
Modeling
Malachite green
Rattan sawdust

ABSTRACT

In this work, the adsorption of malachite green (MG) on rattan sawdust (RSD) was studied at 30 °C. The results indicated that RSD can be used as a low-cost adsorbent for the removal of MG dye from aqueous solutions. Equilibrium data were analyzed by two isotherms, namely the Freundlich isotherm and the Langmuir isotherm. The best fit to the data was obtained with the Langmuir isotherm. The monolayer adsorption capacity of RSD was found to be 62.71 mg/g. The adsorption kinetics can be predicted by the pseudo-first-order model. The mechanism of adsorption was also studied. It was found that for a short time period the rate of adsorption is controlled by film diffusion. However, at longer adsorption times, pore-diffusion controls the rate of adsorption. The amount adsorbed on the outer surface was estimated from the time where film-diffusion stops controlling the adsorption rate.

1. Introduction

Wastewaters discharged from different industries such as the textile, leather tanning, paper production, food technology, hair colorings, etc. are usually polluted by dyes. For example, malachite green is most commonly used for the dyeing of cotton, silk, paper, leather and also in manufacturing of paints and printing inks. Most of the dyes, including malachite green, are toxic and must be removed before discharge into receiving streams.

Adsorption on activated carbons has been proven to be very effective in removing dyes from aqueous solutions. However, activated carbon is still considered expensive and currently the research is focused on the development of low-cost adsorbents for this purpose. Low-cost adsorbents include natural, agricultural, and industrial by-product wastes. They are attractive because of their abundant availability at low or no cost and their good performance in removing dyes from aqueous solutions. Previously several researchers had proved several low-cost materials such as palm ash and chitosan/oil palm ash [1,2], pomelo (*Citrus grandis*) peel [3], sunflower seed hull [4], oil palm trunk fibre [5], durian peel [6] and rice straw-derived char [7], biomass fly ash [8], dried biomass of Baker's yeast [9], water-hyacinth [10] for the removal of dyes from its aqueous solutions. Recently, an extensive list of sorbent literature for dye removal has been compiled by Crini [11].

The objectives of our investigation were to investigate the potential of using rattan sawdust as a low-cost adsorbent to remove malachite green from aqueous solutions, to model the equilibrium and kinetics of the process, and to study the mechanism controlling the rate of adsorption. In the course of studying the mechanism of adsorption, we noticed a relationship between the amount of dye adsorbed on the outer surface of RSD and the total amounts adsorbed at equilibrium. This relationship may be used as a method for estimating the ratio of the outside surface area to the total surface area available for adsorption.

2. Materials and methods

2.1. Adsorbate

The dye, malachite green oxalate, C.I. Basic Green 4, C.I. Classification Number 42,000, chemical formula = $C_{52}H_{54}N_4O_{12}$, MW = 927.00, λ_{max} = 618 nm (measured value) was supplied by Sigma–Aldrich (M) Sdn Bhd, Malaysia. The chemical structure of malachite green oxalate is shown in Scheme 1.

2.2. Adsorbent

The rattan sawdust was collected from a local furniture factory. It was washed several times with distilled water to remove dust like impurities. It was then oven dried at 70 °C for 24 h to constant weight. The dried sample was crushed, sieved to obtain a particle size range of 0.5–1.0 mm, and stored in plastic bottles for later

* Corresponding author. Tel.: +60 4 599 6422; fax: +60 4 594 1013.
E-mail address: chbassim@eng.usm.my (B.H. Hameed).

0304-3894/$ – see front matter © 2008 Elsevier B.V. All rights reserved.
doi:10.1016/j.jhazmat.2008.02.054

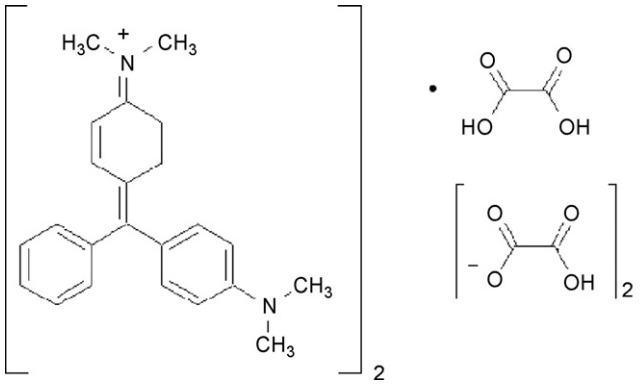

Scheme 1. Chemical structure of malachite green.

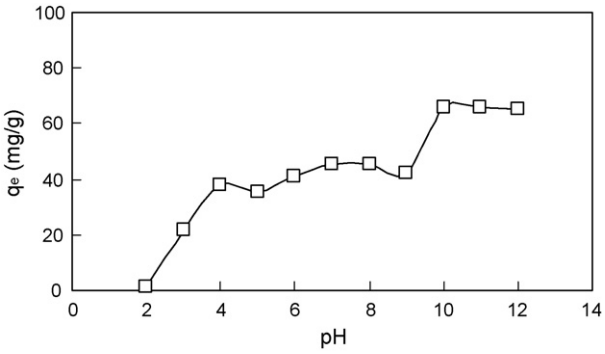

Fig. 1. Effect of pH on equilibrium uptake of MG (W = 0.30 g; V = 0.20 L; C_0 = 100 mg/L).

use. No other chemical or physical treatments were used prior to adsorption experiments.

2.3. Adsorption studies

Batch equilibrium studies were carried out by adding a fixed amount of RSD (0.30 g) into 250-mL Erlenmeyer flasks containing 200 mL of different initial concentrations (25–300 mg/L) of dye solution. The flasks were agitated in an isothermal water-bath shaker at 130 rpm and 30 °C for 210 min until equilibrium was reached. Aqueous samples were taken from the solutions and the adsorbent separated by filtration then the concentrations were analyzed. At time t = 0 and at equilibrium, the dye concentrations were measured by a double beam UV/vis spectrophotometer (Shimadzu, Model UV 1601, Japan) at 618 nm. The amount of equilibrium adsorption, q_e (mg/g), was calculated by:

$$q_e = \frac{(C_0 - C_e)V}{W} \quad (1)$$

where C_0 and C_e (mg/L) are the liquid-phase concentrations of dye at initial and equilibrium, respectively. V (L) is the volume of the solution and W (g) is the mass of dry sorbent used.

To study the effect of solution pH on dye adsorption, 0.30 g of RSD was agitated with 200 mL of dye solution of dye concentration 100 mg/L using water-bath shaker at 30 °C. The experiment was conducted at different pH value ranging from 2 to 12. Agitation was provided for 210 min contact time which is sufficient to reach equilibrium with a constant agitation speed of 130 rpm. At equilibrium, the dye concentrations were measured by a double beam UV/vis spectrophotometer (Shimadzu, Model UV 1601, Japan) at 618 nm. The pH was adjusted by adding a few drops of diluted 0.1N NaOH or 0.1N HCl and was measured by using a pH meter (Ecoscan, EUTECH Instruments, Singapore).

For kinetic studies, 0.30 g of RSD was contacted with 200 mL malachite green solutions of dye concentrations 25–300 mg/L using a water-bath shaker at 30 °C. The agitation speed was kept constant at 130 rpm. At predetermined intervals of time, solutions were analyzed for the final concentration of malachite green.

3. Results and discussion

3.1. Effect of solution pH on dye adsorption

In this work, the effect of pH on the MG adsorption onto RSD was studied while the initial dye concentration, shaking time, amount of RSD and temperature were fixed at 120 mg/L, 210 min, 0.30 g and 30 °C, respectively. The effect of pH on the adsorption of MG by the RSD is presented in Fig. 1. The effect of pH on adsorption of dye was studied within pH range 2–12. Solution pH would affect both aqueous chemistry and surface binding-sites of the adsorbent. The equilibrium sorption capacity was minimum at pH 2 (1.22 mg/g) and increased up to pH 4, reached maximum (38.02–42.53 mg/g) over the initial pH 4–9. Further increase was noticed at pH 10–12. The absence of sorption at low pH can be explained by the fact that at this acidic pH, H^+ may compete with dye ions for the adsorption sites of adsorbent, thereby inhibiting the adsorption of dye. At higher solution pH, the RSD may get negatively charged, which enhances the adsorption of positively charged dye cations through electrostatic forces of attraction. Also a change of solution pH affects the adsorptive process through dissociation of functional groups on the adsorbent surface. Such behavior leads to a shift in equilibrium characteristics of adsorption process. A similar result of pH effect was also reported for the adsorption of methylene blue onto jute fibre carbon [12].

3.2. Equilibrium isotherms

Two commonly used isotherms, Langmuir [13] and Freundlich [14], were employed in the present study. The nonlinear Langmuir and Freundlich isotherms are represented by Eqs. (2) and (3):

$$q_e = K_F C_e^{1/n} \quad (2)$$

$$q_e = \frac{q_m K_a C_e}{1 + K_a C_e} \quad (3)$$

where C_e (mg/L) is the equilibrium concentration, q_e (mg/g) is the amount of dye adsorbed at equilibrium, and q_m (mg/g) and K_a (L/mg) are Langmuir constants related to adsorption capacity and energy of adsorption, respectively. K_F (mg/g)(L/mg)$^{1/n}$ is the Freundlich adsorption constant and $1/n$ is a measure of the adsorption intensity [15].

Fig. 2 shows the fitted equilibrium data in Freundlich and Langmuir isotherms. The fitting results, i.e. isotherm parameters and the coefficients of determination, R^2, are shown in Table 1. It can be seen in Fig. 2 that Langmuir isotherm fits the data better than Freundlich isotherm. This is also confirmed by the high value of R^2 in case of Langmuir (0.999) compared to Freundlich (0.986) and this indicates that the adsorption of MG on RSD takes place as mono-

Table 1
Isotherm constants for MG adsorption on RSD at 30 °C

Langmuir isotherm	
q_m (mg/g)	62.7 ± 1.27
K_a (L/mg)	0.023 ± 0.0014
R^2	0.999
Freundlich isotherm	
K_F	5.88 ± 1.135
n	2.41 ± 0.231
R^2	0.986

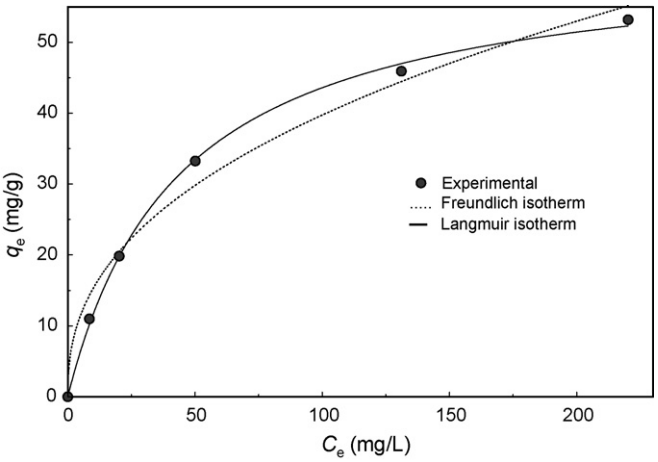

Fig. 2. Isotherm plots for MG adsorption on RSD at 30 °C.

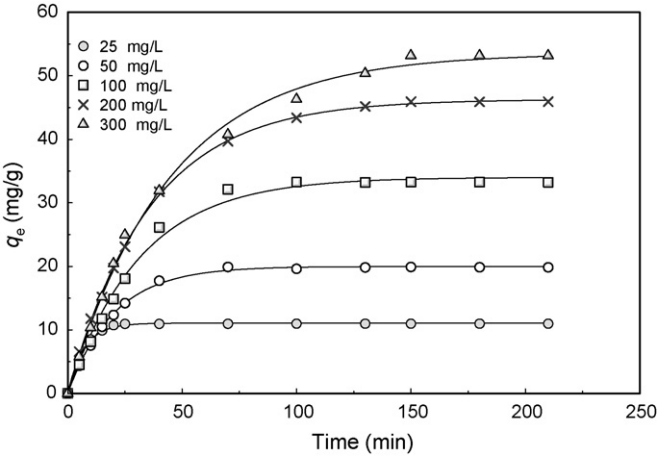

Fig. 4. The fitting of pseudo-first-order model for MG on RSD for different initial concentrations at 30 °C.

layer adsorption on a surface that is homogenous in adsorption affinity.

The RSD adsorbent used in this work had a relatively large adsorption capacity (62.71 mg/g) compared to some other adsorbents reported in the literature, such as bentonite clay (7.72 mg/g) [16] and arundo donax root carbon (8.70 mg/g) [17]. This indicates that RSD is effective to remove MG from aqueous solutions.

The essential characteristics of the Langmuir isotherm can be expressed by a dimensionless constant called the separation factor, K_R, [18] which is defined by

$$K_R = \frac{1}{1 + K_a C_0} \tag{4}$$

where K_a is the Langmuir constant and C_0 is the initial dye concentration (mg/L). K_R values indicate the type of isotherm to be irreversible ($K_R = 0$), favorable ($0 < K_R < 1$), linear ($K_R = 1$), or unfavorable ($K_R > 1$). For adsorption of MG on RSD, K_R values obtained are shown in Fig. 3. The K_R values for the adsorption of MG onto RSD are in the range of 0.128–0.638, indicating that the adsorption is a favorable process and that at high initial MG concentrations the adsorption is nearly irreversible.

3.3. Adsorption kinetics

In order to investigate the adsorption processes of MG on RSD, Lagergren's pseudo-first-order model (Eq. (5)) [19], and Ho's pseudo-second-order model (Eq. (6)) [20] were used

$$q = q_e(1 - e^{-k_1 t}) \tag{5}$$

$$q = \frac{q_e^2 k_2 t}{1 + q_e k_2 t} \tag{6}$$

where q_e (mg/g) is the amount of adsorbate adsorbed at equilibrium, q (mg/g) is the amount of adsorbate adsorbed at time t, k_1 (1/min) is the rate constant of pseudo-first-order adsorption, k_2 (g/mg min) is the rate constant of pseudo-second-order adsorption.

The fittings of the experimental kinetic results to Eqs. (5) and (6) were done by nonlinear regression. The fitting results are shown in Figs. 4 and 5, and the values of the estimated parameters are presented in Table 2. The figures show that the adsorption rate (dq/dt) decreases with time until it gradually approaches the equilibrium state due to the continuous decrease in the driving force ($q_e - q_t$). The plots in Figs. 4 and 5 also demonstrate that the adsorbate uptake, q, increases with increasing the initial concentration. It can be seen in Table 2 that the values of the coefficients of determination, R^2, of the pseudo-first-order model are all higher than those of the second-order model, and also the estimated q_e values from the first-order model are much more accurate. The goodness of fit and the accurate prediction of q_e both indicate that the pseudo-first-order model better describes the adsorption of MG on RSD.

The q versus t plots do not tell much about how close the adsorption system at time t is towards its equilibrium state. For a batch

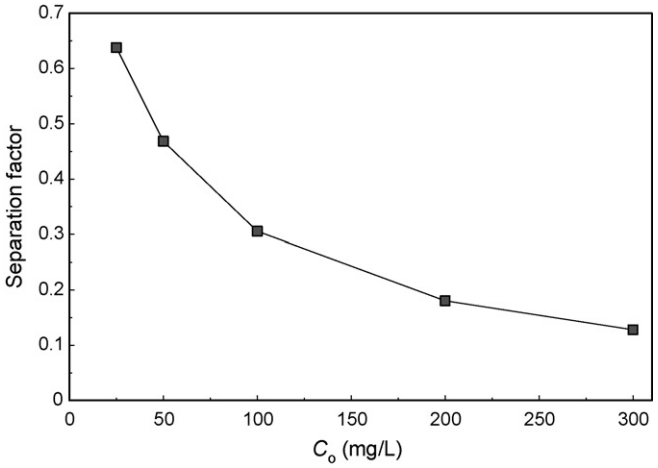

Fig. 3. The separation factor for MG adsorption on RSD at 30 °C.

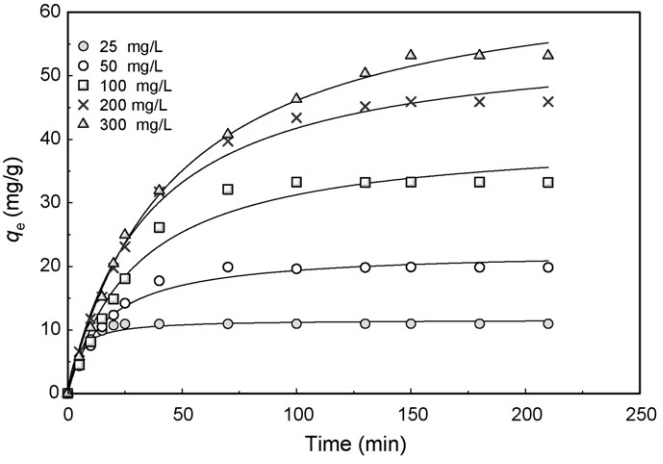

Fig. 5. The fitting of pseudo-second-order model for MG on RSD for different initial concentrations at 30 °C.

Table 2
Kinetic models parameters for the adsorption of MG on RSD at 30 °C and different initial MG concentrations (C_0: mg/L; q_e: mg/g; k_1: 1/min; k_2: g/mg min, K_1: 1/min)

C_0	q_{exp}	Pseudo-first-order			Pseudo-second-order		
		q_e	k_1	R^2	q_e	$k_2 \times 10^3$	R^2
25	11.07	11.07 ± 0.076	0.141 ± 0.0053	0.996	11.64 ± 0.305	22.2 ± 4.73	0.9617
50	20.00	20.00 ± 0.111	0.049 ± 0.0010	0.999	22.46 ± 0.603	2.79 ± 0.370	0.982
100	33.25	34.03 ± 0.509	0.032 ± 0.0016	0.994	40.72 ± 1.745	0.81 ± 0.148	0.976
200	45.92	46.29 ± 0.193	0.029 ± 0.0004	0.999	56.18 ± 1.337	0.51 ± 0.005	0.993
300	53.19	53.54 ± 0.649	0.023 ± 0.0008	0.997	67.30 ± 1.331	0.32 ± 0.002	0.999

adsorption operation, the temporal approach to equilibrium can be illustrated by a plot of the fractional uptake f against time t, where $f = q/q_e$. Fig. 6 shows that the time needed to reach equilibrium increases with increasing the initial MG concentration. It also shows that the fractional uptake f decreases with increasing the initial MG concentration, although this tendency is not so obvious within the high concentration range at short adsorption times. This observation is corroborated by examining the values of k_1 in Table 2, where the values of the rate constant k_1 decrease with increasing the initial concentration of MG from 25 to 300 mg/L. A larger k_1 value implies that it will take a shorter time for the adsorption system to reach the same fractional uptake. Therefore, the trend that k_1 decreases with increasing initial concentration in the range 25–300 mg/L means that it is faster for an adsorption system with a lower initial concentration to reach a specific fractional uptake.

The initial rates of adsorption were calculated from Lagergren's model and the pseudo-second-order model from the equations:

$$h_{0,1} = k_1 q_e \quad (7)$$

$$h_{0,2} = k_2 q_e^2 \quad (8)$$

and the results are plotted in Fig. 7. The general trend seen in the figure is a decrease in the initial rate of adsorption with increasing the initial MG concentration. This is in contradiction to the fact that q_e increases with the increase of C_0 thus increasing the driving force for adsorption, $(q_e - q_0)$, assumed in the derivation of the pseudo kinetic models. Therefore, it is concluded that the initial rate of adsorption is not dependant on chemical reaction, and that the good fit of the pseudo-first-order model to our experimental results should be considered an empirical correlation without any implications regarding the actual mechanism of adsorption.

The rate constants of external mass transfer at the beginning of adsorption were calculated using the plot of C/C_0 against time at different initial MG concentrations shown in Fig. 8. Second-order polynomials were fitted to the data, and $d(C/C_0)/dt$ were calculated from the first derivative of the polynomials at $t = 0$. The values of

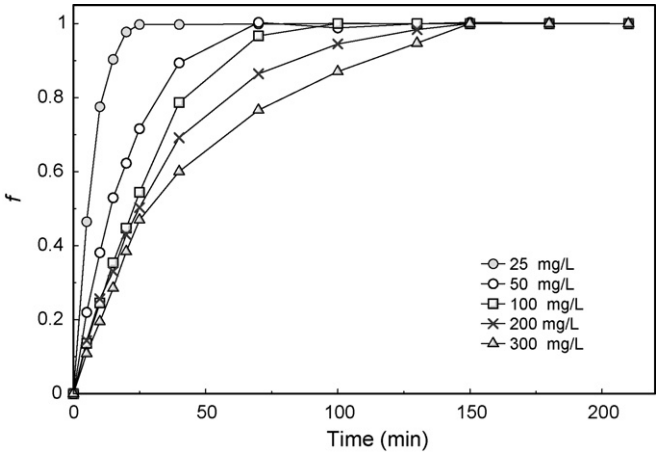

Fig. 6. The fractional approach to equilibrium with time for different initial MG concentrations 30 °C.

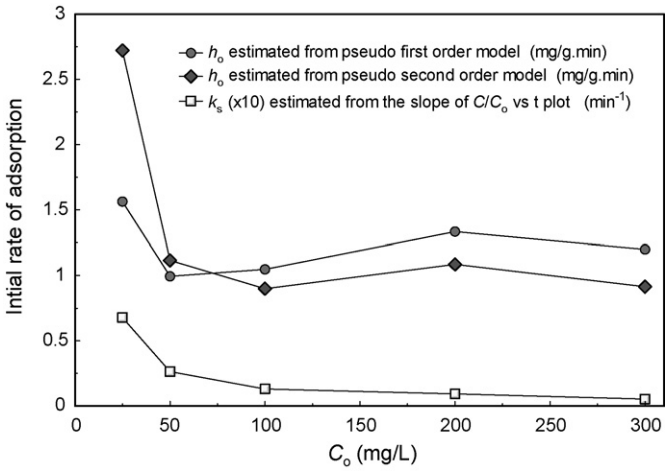

Fig. 7. The variation of the initial rate of adsorption with the initial MG concentration.

the mass transfer constant, k_s (1/min) are presented in Table 3 and plotted in Fig. 8. It is observed that unlike $h_{0,1}$ and $h_{0,2}$, the values of k_s decrease steadily with the increase of C_0. The estimation of the initial rate of adsorption by k_s is more reliable than $h_{0,1}$ and $h_{0,2}$ for two reasons:

- k_s is calculated directly from the temporal change of C/C_0 without any theoretical assumptions about the mechanism of adsorption;
- k_s is precisely calculated at $t = 0$, from fitting C/C_0 values for a short period at the beginning of adsorption, while $h_{0,1}$ and $h_{0,2}$ are calculated from estimates of q_e and k that are obtained from regression and are affected by the change of q with t throughout the entire adsorption period.

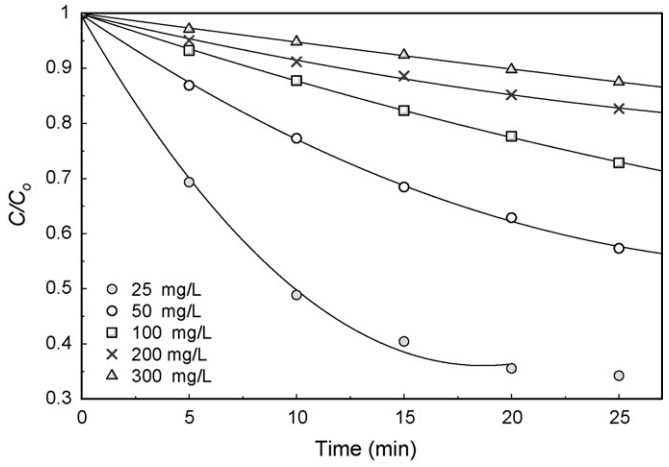

Fig. 8. The variation of the C/C_0 with time at different initial MG concentration.

Table 3
Diffusion coefficients for adsorption of MG on RSD at 30 °C and different initial concentrations (C_0: mg/L; k_s: 1/min; D_p: cm^2/min; k_i: mg/g $min^{0.5}$; diffusion period: min)

C_0	$k_s \times 100$	$k_{i,1}$ [b]	$D_p \times 10^6$	$k_{i,2}$	Pore diffusion period[a]
25	6.79 ± 0.383	1.36	1.84	–	11.2–21.4
50	2.64 ± 0.100	2.31	1.64	–	32.1–57.6
100	1.30 ± 0.045	3.23	1.15	–	41.1–75.9
200	0.93 ± 0.072	3.90	0.88	1.265	39.9–143.7
300	0.53 ± 0.026	3.18	0.44	–	47.1–149.8

[a] Estimated from the start of the second linear segment to the end of the third linear segment in the pore-diffusion plot.
[b] Uncertainty analysis can not be applied because some of the slopes were calculated from only 2 data points.

The decrease of k_s with increasing dye concentration was reported by Allen et al. for the adsorption of basic red 22 and basic yellow 21 on peanut hulls. [21]. They attributed this trend to the competition for available surface area for adsorption between the large numbers of dye molecules, which seems to have more influence on the initial rate of adsorption than the increasing driving force caused by higher dye concentration.

3.4. Mechanism of adsorption

At the present time, the models of Boyd [22] and Webber [23] are widely used for studying the mechanism of adsorption.

Boyd's model determines whether the main resistance to mass transfer is in the thin film (boundary layer) surrounding the adsorbent particle, or in the resistance to diffusion inside the pores. This model is expressed as

$$f = 1 - \frac{6}{\pi^2}\sum_{n=1}^{\infty}\frac{1}{n^2}\exp(-n^2\mathrm{Bt}) \quad (9)$$

where f is the fractional attainment of equilibrium, at different times, t, and Bt is a function of f.

$$f = \frac{q_t}{q_e} \quad (10)$$

where q_t and q_e (mg/g) are the dye uptake at time t and at equilibrium, respectively.

From Eq. (9), it is not possible to calculate the values of B for each fraction adsorbed. By applying the Fourier transform and then integration, Reichenberg [24] obtained the following approximations:

$$\text{for } F \text{ values} > 0.85 \quad \mathrm{Bt} = -0.4977 - \ln(1-F) \quad (11)$$

$$\text{and for } F \text{ values} < 0.85 \quad \mathrm{Bt} = \left(\sqrt{\pi} - \sqrt{\pi - \left(\frac{\pi^2 F}{3}\right)}\right)^2 \quad (12)$$

B, can be used to calculate the effective diffusion coefficient, D_i (cm^2/s), from the equation:

$$B = \frac{\pi^2 D_i}{r^2} \quad (13)$$

where r is the radius of the adsorbent particle assuming spherical shape.

Eqs. (10)–(13) can be used in predicting the mechanism of the adsorption process. This is done by plotting Bt against time, if the plot is linear and passes through the origin then pore-diffusion controls the rate of mass transfer. If the plot is nonlinear or linear but does not pass through the origin, then it is concluded that film-diffusion or chemical reaction control the adsorption rate.

Fig. 9 shows the Boyd plots for the first 40 min of MG adsorption on RSD at 30 °C. The plots show a nonlinear segment at short adsorption times, which means that the experimental data does not follow Eqs. (11) and (12) and thus pore diffusion does not control the rate of adsorption in the initial period. This suggests that film-diffusion or chemical reaction controls the rate of adsorption during this period.

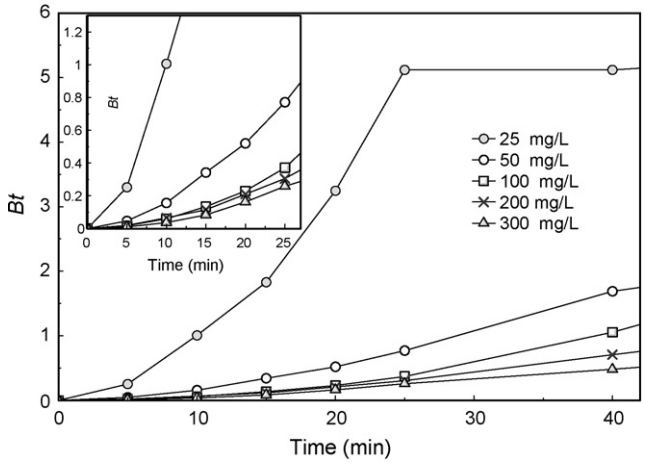

Fig. 9. Boyd plots for MG adsorption on RSD at 30 °C and different initial MG concentrations.

On the other hand, Webber's pore-diffusion model was derived from Fick's second law of diffusion. The pore diffusion parameter, k_i (mg/g $min^{0.5}$) is defined by:

$$q = k_i t^{0.5} \quad (14)$$

where q is the amount adsorbed (mg/g) at time t. It can be seen from Eq. (14) that if pore-diffusion is the rate limiting step, then a plot of q against $t^{0.5}$ must give a straight line with a slope that equals k_i and an intercept equal to zero. Fig. 10 shows the pore diffusion plot of MG adsorption on RSD at 30 °C. It is clear that the plots are multilinear, having at least three linear segments. The software package NCSS [25] was used to fit the data to the model by the method of piecewise linear regression. The regression results are presented in Table 3. For all the multilinear plots in Fig. 10, the regression results of the first linear segments estimated intercept values that are significantly different from zero. These intercept values corroborate the conclusion from the Boyd plots that pore diffusion does not control the overall rate of adsorption at this early stage. Therefore, it is confirmed that the first linear segment represents film-diffusion (or chemical reaction), and that the following linear segments represent pore-diffusion and equilibrium.

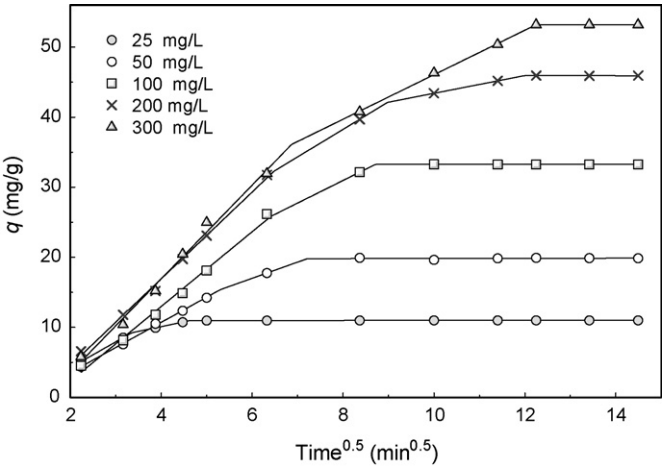

Fig. 10. Intraparticle diffusion plot for the adsorption at 30 °C and different initial MG concentrations.

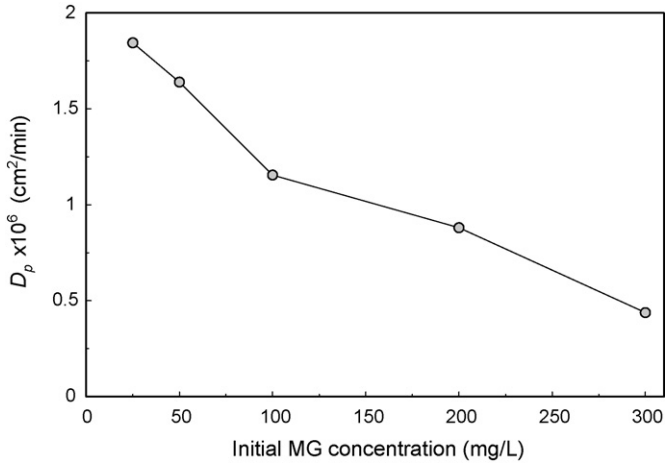

Fig. 11. The variation of pore diffusion coefficient with the initial MG concentration.

In cases where two pore diffusion periods are found, then two pore diffusion parameters, $k_{i,1}$ and $k_{i,2}$, can be calculated from the slopes of the two corresponding lines. These rate parameters $k_{i,1}$ and $k_{i,2}$ represent the diffusion of MG in pores that have two distinct sizes (macropores and mesopores) [26]. Usually, a decrease in value of k_i from macropore to mespore diffusion is a normal consequence of reducing the relative free path for diffusion in each pore size.

The results of piecewise linear regression shown in Fig. 10 and Table 3 also suggest that for all initial MG concentrations except 200 mg/L, there is only one pore diffusion period. This period starts after the end of a film-diffusion (or chemical reaction) controlled period, represented by the first linear segment, and continues until equilibrium is established. Only for C_0 = 200 mg/L there is evidence on the existence of two consecutive pore-diffusion controlled periods before equilibrium. This does not necessarily prove that for other initial concentrations the mechanism of adsorption has only one pore-diffusion period, it is possible that our data for these concentrations do not contain enough data points during the second period of pore diffusion, thus lumping the two pore-diffusion periods and producing one k_i value.

It is observed in Table 3 that an increase in the initial MG concentration from 25 to 200 mg/L increases the pore diffusion rate parameter $k_{i,1}$ from 1.36 to 3.90 mg/g min$^{0.5}$, but a further increase of C_0 to 300 mg/L decreases $k_{i,1}$ to 3.18 mg/g min$^{0.5}$. This discrepancy is resolved by calculating the diffusivity of MG in the pores, D_p (cm^2/min), from the relation [27].

$$k_i = \frac{6q_e}{r}\sqrt{\frac{D_p}{\pi}}. \quad (15)$$

The values of D_p are given in Table 3 and the relation between D_p and C_0 is shown in Fig. 11 and it is obvious that D_p decreases almost linearly with the increase in C_0. This can be explained by the increased resistance to diffusion at high MG concentration caused by the repulsion between charged MG molecules. Similar results on the relationship between dye concentration and intraparticle adsorption rate were reported by Ho and McKay for the adsorption of Chrysordine on Sphagnum Moss peat [28].

4. Conclusions

The present study shows that RSD can be used as an adsorbent for the removal of MG dye from aqueous solutions. The amount of dye adsorbed was found to vary with initial of MG concentration and contact time. The Langmuir adsorption isotherm was found to have the best fit to the experimental data, suggesting monolayer adsorption on a homogenous surface. The adsorption kinetics can be predicted by the pseudo-first-order model. It was found that for a short time period the rate of adsorption is controlled by film diffusion. However, at longer adsorption times, pore-diffusion controls the rate of adsorption.

Acknowledgements

The authors acknowledge the research grant provided by the Universiti Sains Malaysia under the Research University (RU) Scheme (Project No: 1001/PJKIMIA/814005).

References

[1] A.A. Ahmad, B.H. Hameed, N. Aziz, Adsorption of direct dye on palm ash: kinetic and equilibrium modeling, J. Hazard. Mater. 141 (2007) 70–76.
[2] M. Hasan, A.L. Ahmad, B.H. Hameed, Adsorption of reactive dye onto cross-linked chitosan/oil palm ash composite beads, Chem. Eng. J. 136 (2008) 164–172.
[3] B.H. Hameed, D.K. Mahmoud, A.L. Ahmad, Sorption of basic dye from aqueous solution by pomelo (*Citrus grandis*) peel in a batch system, Colloids Surf. A: Physicochem. Eng. Aspects 316 (2008) 78–84.
[4] B.H. Hameed, Equilibrium and kinetic studies of methyl violet sorption by agricultural waste, J. Hazard. Mater. 154 (2008) 204–212.
[5] B.H. Hameed, M.I. El-Khaiary, Batch removal of malachite green from aqueous solutions by adsorption on oil palm trunk fibre: equilibrium isotherms and kinetic studies, J. Hazard. Mater. 154 (2008) 237–244.
[6] B.H. Hameed, H. Hakimi, Utilization of durian (*Durio zibethinus Murray*) peel as low cost sorbent for the removal of acid dye from aqueous solutions, Biochem. Eng. J. 39 (2008) 338–343.
[7] B.H. Hameed, M.I. El-Khaiary, Kinetics and equilibrium studies of malachite green adsorption on rice straw-derived char, J. Hazard. Mater. 153 (2008) 701–708.
[8] P. Pengthamkeerati, T. Satapanajaru, O. Singchan, Sorption of reactive dye from aqueous solution on biomass fly ash, J. Hazard. Mater. 153 (2008) 1149–1156.
[9] J.Y. Farah, N.Sh. El-Gendy, L.A. Farahat, Biosorption of Astrazone Blue basic dye from an aqueous solution using dried biomass of Baker's yeast, J. Hazard. Mater. 148 (2007) 402–408.
[10] M.I. El-Khaiary, Kinetics and mechanism of adsorption of methylene blue from aqueous solution by nitric-acid treated water-hyacinth, J. Hazard. Mater. 147 (2007) 28–36.
[11] G. Crini, Non-conventional low-cost adsorbents for dye removal: a review, Bioresour. Technol. 97 (2006) 1061–1085.
[12] S. Senthilkumaar, P.R. Varadarajan, K. Porkodi, C.V. Subbhuraam, Adsorption of methylene blue onto jute fiber carbon: kinetics and equilibrium studies, J. Colloid Interf. Sci. 284 (2005) 78–82.
[13] I. Langmuir, The constitution and fundamental properties of solids and liquids, J. Am. Chem. Soc. 38 (11) (1916) 2221–2295.
[14] H.M.F. Freundlich, Over the adsorption in solution, J. Phys. Chem. 57 (1906) 385–470.
[15] Y.S. Ho, G. McKay, Sorption of dye from aqueous solution by peat, Chem. Eng. J. 70 (1998) 115–124.
[16] S.S. Tahir, N. Rauf, Removal of a cationic dye from aqueous solutions by adsorption onto bentonite clay, Chemosphere 63 (2006) 1842–1848.
[17] J. Zhang, Y. Li, C. Zhang, Y. Jing, Adsorption of malachite green from aqueous solution onto carbon prepared from Arundo donax root, J. Hazard. Mater. 150 (2008) 774–782.
[18] T.W. Weber, R.K. Chakravorti, Pore and solid diffusion models for fixed-bed adsorbers, AIChE J. 20 (2) (1974) 228–238.
[19] S. Lagergren, About the theory of so-called adsorption of soluble substances, K. Sven. Vetenskapsakad. Handl. 24 (4) (1898) 1–39.
[20] Y.S. Ho, Adsorption of heavy metals from waste streams by peat, Ph.D. Thesis, University of Birmingham, Birmingham, UK, 1995.
[21] S.J. Allen, Q. Gan, R. Matthews, P.A. Johnson, Ind. Eng. Chem. Res. 44 (2005) 1942–1949.
[22] G.E. Boyd, A.W. Adamson, L.S. Myers Jr., The exchange adsorption of ions from aqueous solutions by organic zeolites. Part II. Kinetics, J. Am. Chem. Soc. 69 (1947) 2836–2848.
[23] W.J. Weber Jr., J.C. Morris, Kinetics of adsorption on carbon from solution, J. Sanitary Eng. Div. Proceed. Am. Soc. Civil Eng. 89 (1963) 31–59.
[24] D. Reichenberg, Properties of ion exchange resins in relation to their structure. Part III. Kinetics of exchange, J. Am. Chem. Soc. 75 (1953) 589–598.
[25] J. Hintze, NCSS, PASS, and GESS, NCSS, Kaysville, Utah, 2006.
[26] S.J. Allen, G. McKay, K.Y.H. Khader, Intraparticle diffusion of a basic dye during adsorption onto sphagnum peat, Environ. Pollut. 56 (1989) 39–50.
[27] X. Yang, B. Al-Duri, Kinetic modeling of liquid-phase adsorption of reactive dyes on activated carbon, J. Colloid Interf. Sci. 287 (1) (2005) 25–34.
[28] Y.S. Ho, G. McKay, The kinetics of sorption of basic dyes from aqueous solution by Sphagnum Moss peat, Canadian, J. Chem. Eng. 76 (1998) 822–827.